

Effect of Dy substitution on the microstructure and magnetic properties of nanograin Nd-Fe-B single-phase alloys

Zhi-an Chen, Ji Luo, and Zhi-meng Guo

School of Materials Science and Engineering, University of Science and Technology Beijing, Beijing 100083, China

(Received: 15 May 2009; revised: 18 June 2009; accepted: 27 June 2009)

Abstract: Nanocrystalline single-phase alloys with the nominal compositions (at%) of $\text{Nd}_{12.3-x}\text{Dy}_x\text{Fe}_{79.7}\text{Zr}_{0.8}\text{Nb}_{0.8}\text{Cu}_{0.4}\text{B}_{6.0}$ ($x=0, 0.5, 1.5$, and 2.5) were prepared by melt-spinning and subsequent annealing. X-ray diffraction analysis shows that the as-spun ribbons were mainly composed of the amorphous phase. A slight content of Dy stabilizes the amorphous phase during annealing treatment. The grain size becomes smaller and the coercivity of the annealed ribbon is gradually improved with the increase of Dy content. Excessive Dy is harmful to the remanence. It is found that no intergranular phase exists between the grains by high-resolution transmission electron microscopy, and the grain boundaries are crystallographically coherent in the optimally annealed sample. The optimum magnetic properties of remanence ($J_r=1.09$ T), coercivity ($H_{ci}=1048$ kA/m), and maximum magnetic energy product $((BH)_m=169.5$ kJ/m³) are obtained from the $x=0.5$ ribbon in a post heat-treated state (700°C, 10 min).

Keywords: NdFeB magnets; dysprosium; nanocrystalline; amorphous; grain size; magnetic properties

1. Introduction

Nanograin NdFeB hard magnets have attracted much attention due to the effect of remanence (J_r) enhancement induced by the intergranular exchange interaction [1-4]. Some researches have been carried out on the effect of Dy substitution in the Nd-Fe-B system [5-6]. The results show that the magnetocrystalline anisotropy field (H_A) is improved since the H_A of $\text{Dy}_2\text{Fe}_{14}\text{B}$ ($H_A=12576.8$ kA/m) is much higher than that of $\text{Nd}_2\text{Fe}_{14}\text{B}$ ($H_A=5572$ kA/m) [7]. On the other hand, Dy substitution can optimize the microstructure of the $\text{Nd}_2\text{Fe}_{14}\text{B}$ matrix and decrease the grain size, which are important for producing magnets with high coercivity (H_{ci}) [8-9].

Jang *et al.* [10] have researched the effect of Dy substitution on $\text{Nd}_2\text{Fe}_{14}\text{B}$ nanocomposites. They found that a small amount of Dy can enhance the nucleation rate, which is beneficial for obtaining the fine and uniform $\text{Nd}_2\text{Fe}_{14}\text{B}$ grains. However, researches on Dy substitution in Nd-Fe-B single-phase nanograin alloys are seldom reported. To make clear the role of Dy substitution and effectively develop the

magnetic performance of this kind of magnets, this work focused on the effect of Dy substitution on the microstructure and magnetic properties of $\text{Nd}_2\text{Fe}_{14}\text{B}$ single-phase nanograin magnets.

2. Experimental

Alloy ingots with nominal compositions (at%) of $\text{Nd}_{12.3-x}\text{Dy}_x\text{Fe}_{79.7}\text{Zr}_{0.8}\text{Nb}_{0.8}\text{Cu}_{0.4}\text{B}_{6.0}$ ($x=0, 0.5, 1.5$, and 2.5) were prepared using commercial grade materials by vacuum induction melting, they were named as A ($x=0$), B ($x=0.5$), C ($x=1.5$), and D ($x=2.5$) for short. The over-quenched ribbons were produced by melt-spinning onto the surface of a copper wheel rotating at the speed of 22 m/s in a high-purity Ar atmosphere. The ribbons selected (40-50 μm in thickness) were annealed at 550-800°C for 10 min to optimize crystallization and improve the permanent magnetic properties. The phase composition of the ribbons was determined by X-ray diffraction and high temperature X-ray diffraction with Cu K α radiation. The crystallization behavior was examined by differential scanning calorimetry (DSC). The magnetic properties of the ribbons were measured with a vi-

Corresponding author: Zhi-an Chen E-mail: alvincza@gmail.com

© University of Science and Technology Beijing and Springer-Verlag Berlin Heidelberg 2010

brating sample magnetometer (LDJ9600 VSM) in the field up to 1.6 MA/m at room temperature. The microstructures were observed by high-resolution transmission electron microscopy (HR-TEM JEM2010) with thin foils prepared by ion-beam thinning.

3. Results and discussion

3.1. Phase composition and crystallization behavior of the as-spun ribbons

Fig. 1 shows the DSC curves of the as-spun ribbons with different Dy contents. Comparing with the curve of the Dy-free ($x=0$) sample in Fig. 1(b), the substitution of 1.5at% Dy is observed to retard the crystallization by 35°C, implying that a slight amount of Dy can stabilize the amorphous phase during annealing treatment.

An as-spun C ($x=1.5$) ribbon was analyzed by the high-temperature X-ray instrument. Fig. 2 shows the diffractograms of the C ($x=1.5$) ribbon at 20, 600, 700, and 800°C. It can be seen that the sample consists of the amorphous phase at room temperature. The peaks corresponding to the hard magnetic $\text{Nd}_2\text{Fe}_{14}\text{B}$ phase are enhanced when the temperature increases to 600°C. Combined with Fig. 1(a), the C ($x=1.5$) as-spun sample should be intensively crystallized around 600°C. With a further increase in temperature to 800°C, the width of the peak becomes narrower, indicating the grains have grown up.

3.2. Relationship between Dy content and magnetic properties of annealed ribbons

Fig. 3 shows the coercivities of samples A ($x=0$), B ($x=0.5$), C ($x=1.5$), and D ($x=2.5$) annealed at different temperatures. When the Dy content is not larger than 0.5at%, with the increase of annealing temperature from 600 to 800°C, the coercivities first improve, and then decrease. When the Dy content is larger than 0.5at%, however, the

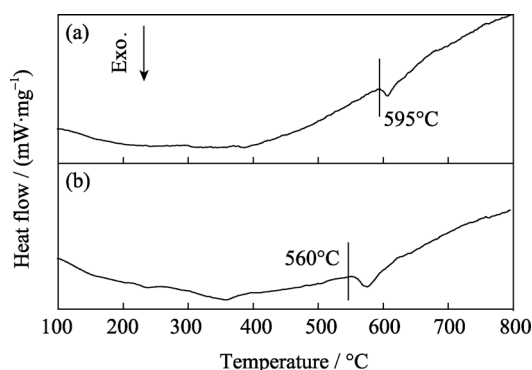


Fig. 1. DSC curves of the as-spun ribbons with different Dy contents: (a) $x=1.5$; (b) $x=0$.

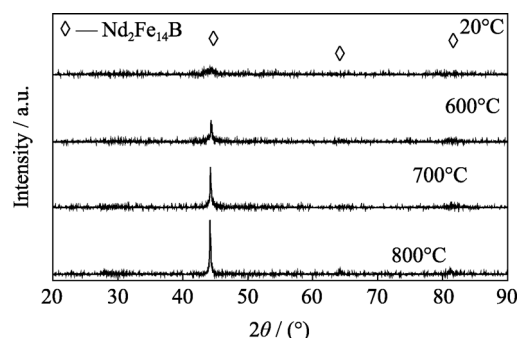


Fig. 2. High temperature X-ray diffraction patterns of the C ($x=1.5$) as-spun ribbon.

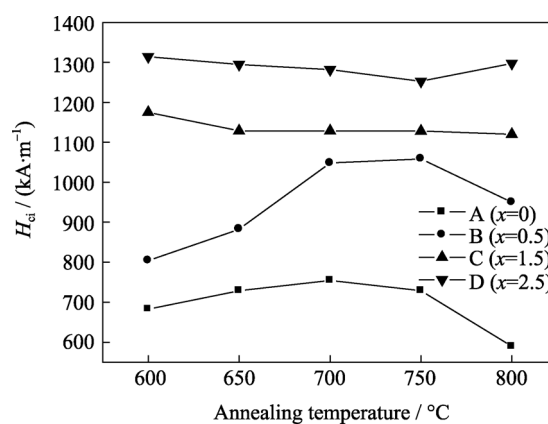


Fig. 3. Coercivities of the A ($x=0$), B ($x=0.5$), C ($x=1.5$), and D ($x=2.5$) ribbons annealed at different temperatures.

coercivities do not change very much at different annealing temperatures. In addition, with the increase of Dy content, the coercivities are gradually enhanced at the same annealing temperature.

TEM images of the specimens in a post heat-treated state (700°C, 10 min) with different Dy contents are observed in Fig. 4. The grains become more regular, and the grain size becomes smaller from 40 to 20 nm with an increase in Dy content from 0at% to 1.5at%. This implies that a slight amount of Dy effectively unifies the grains and suppresses the growth of the grains during the heat treatment. It is well known that the coercivity is very sensitive to the grain shape and grain size [11]. To increase the coercivity, the uniform microstructure must be established. On the other hand, when the grain size is smaller than 40 nm, the fine grains and uniform distribution greatly enhance the exchange-coupling interaction, which can weaken the H_{ci} values of the single $\text{RE}_2\text{Fe}_{14}\text{B}$ phase alloy [12-13].

According to some literatures [14-15], the magnetocrystalline anisotropy field (H_A) of the $\text{Nd}_2\text{Fe}_{14}\text{B}$ single crystal is about 5600 kA/m, and that of the $\text{Dy}_2\text{Fe}_{14}\text{B}$ single crystal is

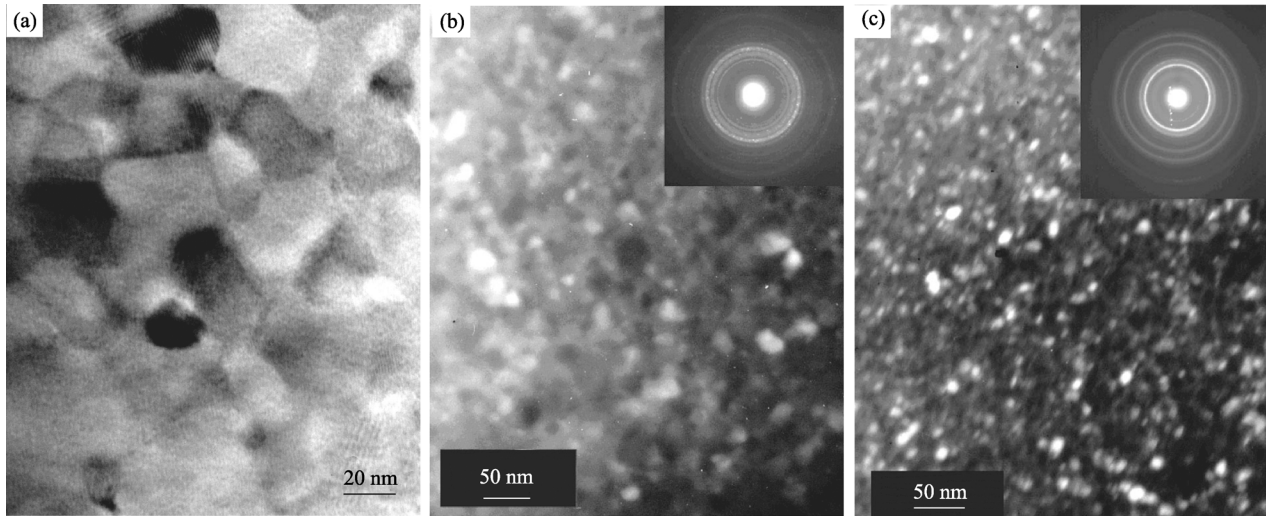


Fig. 4. TEM images of the annealed ribbons: (a) A ($x=0$); (b) B ($x=0.5$); (c) C ($x=1.5$).

about 12600 kA/m. What is more, the $\text{Nd}_2\text{Fe}_{14}\text{B}$ phase and the $\text{Dy}_2\text{Fe}_{14}\text{B}$ phase are totally mutual soluble. So, when the content of Dy substitution is enhanced, the H_A of the $(\text{Nd}, \text{Dy})_2\text{Fe}_{14}\text{B}$ alloy should be improved. On the basis of the values above, the H_A of the $(\text{Nd}, \text{Dy})_2\text{Fe}_{14}\text{B}$ alloy will be increased by 70 kA/m with 1at% Dy substitution. This also means that Dy atoms probably has replaced the lattice point of Nd atoms in the $\text{Nd}_2\text{Fe}_{14}\text{B}$ unit cell. This is one of the important reasons that increasing the Dy content effectively enhances the magnetic coercivity in Fig. 3.

The demagnetization curves of the annealed ribbons with different Dy contents are shown in Fig. 5. When the Dy content increases from 0at% to 2.5at%, although H_{ci} is improved from 683 to 1315 kA/m, J_r obviously becomes worse from 1 to 0.6 T. Interestingly, there are two steps during this decreasing process. First, the remanence does not even change with an increase of Dy content from 0at% to 0.5at%. However, when the amount of Dy further increases to

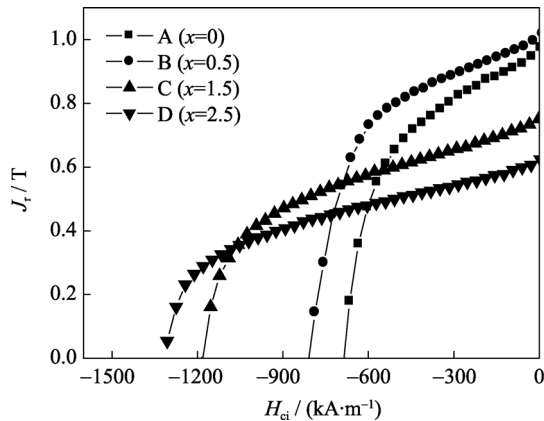


Fig. 5. Demagnetization curves of A, B, C, and D ribbons annealed at 600°C for 10 min.

1.5at%, the remanence quickly becomes worse. The effect of Dy on decreasing the grain size which leads to a stronger exchange coupling is discussed above. Dy substitution also reduces the saturation magnetization (J_s) and J_r , since the magnetic moment of Dy couples is antiparallel to both Nd and Fe moments [16]. With further Dy addition, the effect of Dy on reducing J_s and J_r becomes stronger. So the remanence decreases.

The best magnetic coercivity is 1315 kA/m obtained from the D ($x=2.5$) ribbon in a post heat-treated state (600°C, 10 min). However, the optimum magnetic properties with $J_r=1.09$ T, $H_{ci}=1048$ kA/m, and maximum magnetic energy product $(BH)_m=169.5$ kJ/m³ are obtained from the B ($x=0.5$) ribbon annealed at 700°C for 10 min, which is also the sample with the best remanence (1.09 T). So in this series of materials, a poorer remanence means a worse maximum magnetic energy product.

3.3. Microstructure of the annealed Dy-substituted specimen

HR-TEM images of the C ($x=1.5$) ribbon in a post heat-treated state (700°C, 10 min) are observed in Fig. 6. By the use of the software Digital Micrograph, the corresponding Fourier filtered image in Fig. 7 is made.

There mainly are three parts in the TEM image: grain 1, grain 2, and grain 3. The crystal lattice is very clear not only inside the grains but also on the grain boundaries. It suggests that the crystallization is perfectly complete. Moreover, no intergranular phase is found between the grains. The grain boundaries are totally crystallographically coherent. This is different from the structure of the sintered NdFeB magnets, whose coercivity dramatically depends on the Nd-rich phase

between and around the grains. Fig. 7 shows the Fourier filtered image corresponding to the boundary of grain 1 and grain 3 in Fig. 6. The completely coherent grain boundary in Fig. 7 also proves that the coercivity mechanism in this

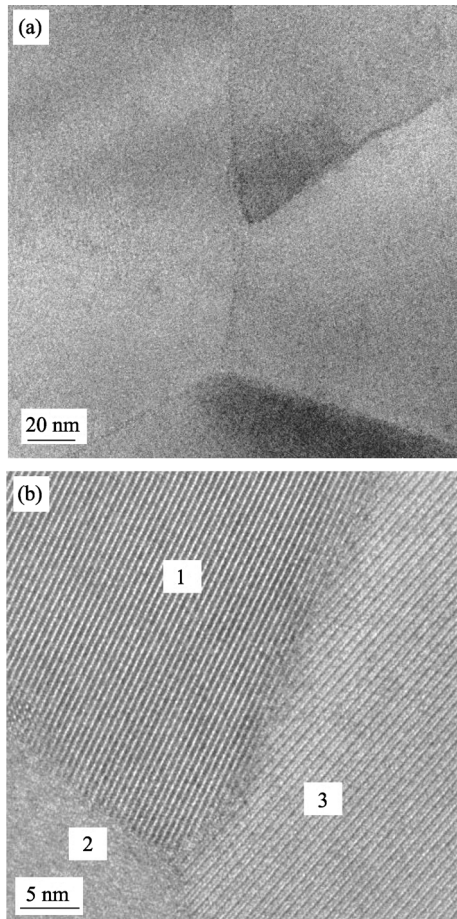


Fig. 6. HR-TEM images of the C ($x=1.5$) annealed ribbon: (a) low amplification; (b) high amplification.

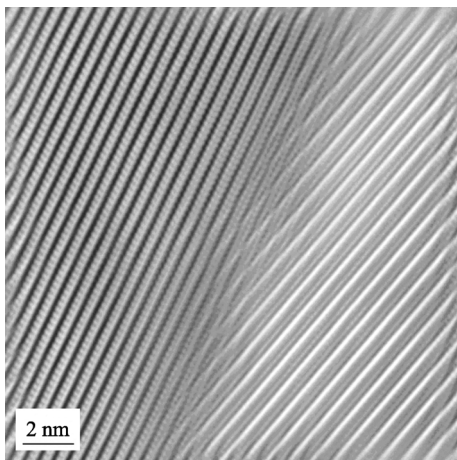


Fig. 7. Fourier filtered image corresponding to the grain boundary of 1 and 3 in Fig. 6.

series of materials is not similar to the traditional one in the sintered magnets. The magnetic coercivity is probably realized by the effect of the magnetic exchange-coupling interaction between grains.

4. Conclusions

(1) A slight content of Dy stabilizes the amorphous phase during the annealing treatment.

(2) When the Dy content is not larger than 0.5at%, with an increase of annealing temperature from 60 to 800°C, the coercivities first improve, and then decrease. When the Dy content is larger than 0.5at%, the coercivities do not change much with the increase of annealing temperature. At the same post heat-treated temperature, the coercivities are gradually improved when the Dy content is enhanced. The highest magnetic coercivity is 1315 kA/m obtained from the D ($x=2.5$) ribbon in a post heat-treated state (600°C, 10 min).

(3) The optimum magnetic properties of $J_r=1.09$ T, $H_{ci}=1048$ kA/m, and $(BH)_m=169.5$ kJ/m³ are obtained by annealing the melt-spun $Nd_{11.8}dy_{0.5}Fe_{79.7}Zr_{0.8}Nb_{0.8}Cu_{0.4}B_{6.0}$ ribbon at 700°C for 10 min. Excessive Dy weakens the remanence due to the lower J_s of $Dy_2Fe_{14}B$.

(4) No intergranular phase is found in the optimally annealed sample. The grain boundaries are totally crystallographically coherent. The magnetic coercivity is probably realized by the exchange coupling interaction rather than the intergranular phase.

References

- [1] M. Ghidini, G. Asti, R. Pellicelli, *et al.*, Hard-soft composite magnets, *J. Magn. Magn. Mater.*, 316(2007), No.2, p.159.
- [2] H. Chiriac, N. Lupu, L. Stoleriu, *et al.*, Experimental and micromagnetic first-order reversal curves analysis in NdFeB-based bulk “exchange spring”-type permanent magnets, *J. Magn. Magn. Mater.*, 316(2007), No.2, p.177.
- [3] D.N. Brown, Z. Chen, P. Guschl, and P. Campbell, Developments with melt spun RE-Fe-B powder for bonded magnets, *J. Magn. Magn. Mater.*, 303(2006), No.2, p.371.
- [4] H.W. Kwon and G.C. Hadjipanayis, Magnetic and microstructural study of hybrid magnet consisting of R-rich and R-lean Nd-Fe-B alloys, *J. Magn. Magn. Mater.*, 310(2007), No.2, p.2575.
- [5] W.F. Miao, J. Ding, P.G. McCormick, and R. Street, Magnetic behaviour of mechanically milled $(Nd_{1-x}Dy_x)_8Fe_{88}B_4$, *J.*

- Magn. Magn. Mater.*, 175(1997), No.3, p.304.
- [6] X. Fang, Y. Shi, and D.C. Jiles, Modeling of magnetic properties of heat treated Dy-doped NdFeB particles bonded in isotropic and anisotropic arrangements, *IEEE Trans. Magn.*, 34(1998), No.4, p.1291.
- [7] S.G. Kim, M.J. Kim, K.S. Ryu, *et al.*, Effect of Dy on magnetic properties of α -Fe/Nd₂Fe₁₄B type alloy, *IEEE Trans. Magn.*, 36(1999), No.5, p.3316.
- [8] Z.W. Liu and H.A. Davies, Elevated temperature study of nanocrystalline (Nd/Pr)-Fe-B hard magnetic alloys with Co and Dy additions, *J. Magn. Magn. Mater.*, 290(2005), No.2, p.1230.
- [9] L.M. Liu, Y.L. Shi, and X.M. Zhao, Magnetic properties and curie temperature of nanocomposite (Nd_{0.7}Dy_{0.3})₈Fe₈₇B₅, *J. Hebei Norm Univ. Nat. Sci. Ed.*, 29(2005), No.4, p.261.
- [10] T. Jang and Y.S. Kim, Effect of small dysprosium additions on the coercivity of melt-spun Nd-Fe-C alloys, *IEEE Trans. Magn.*, 36(1999), No.5, p.3310.
- [11] Y.H. Gao, J.H. Zhu, Y.Q. Weng, *et al.*, The enhanced exchange coupled interaction in nanocrystalline Nd₂Fe₁₄B/Fe₃B+ α -Fe alloys with improved microstructure, *J. Magn. Magn. Mater.*, 191(1999), No.1, p.146.
- [12] R.J.I. Betancourt and H.A. Davies, Effect of grain size on the magnetic properties of nanophase REFeB alloys, *J. Magn. Magn. Mater.*, 246(2002), No.1-2, p.6.
- [13] A. Manaf, R.A. Buckley, H.A. Davies, and M. Leonowicz, Enhanced magnetic properties in rapidly solidified Nd-Fe-B based alloys, *J. Magn. Magn. Mater.*, 101(1991), No.1, p.360.
- [14] M. Sagawa, S. Fujimura, and H.Y. Yamamoto, Magnetic properties and microstructure of rare Earth-Iron-Boron permanent magnet materials, [in] *Proceeding of the 4th International Symposium on Anisotropy and Coercivity in Rare Earth-Transition Metal Alloys*, Ohio Dayton, 1985, p.587.
- [15] K.H.J. Buschow, New developments in hard magnetic materials, *Rep. Prog. Phys.*, 54(1991), No.9, p.1123.
- [16] Z.W. Liu, Y. Liu, P.K. Deheri, *et al.*, Improving permanent magnetic properties of rapid solidified nanophase RE-TM-B alloys by compositional modification, *J. Magn. Magn. Mater.*, 321(2009), No.15, p.2290.